



LABORATORI NAZIONALI DI FRASCATI

SIS – Pubblicazioni

LNF-94/031 (P)

9 Giugno 1994

ROM2F 94/12

The Hadronic Vacuum Polarization Contribution to the Muon $g-2$ in the Quark-Resonance Model

E. Pallante*

INFN – Laboratori Nazionali di Frascati, P.O. Box 13, I-00044 Frascati (Roma) Italy

Abstract

The hadronic vacuum polarization contribution to the anomalous magnetic moment of the muon is parametrized by using the quark-resonance model formulated in^[1]. In this context a recent prediction obtained within the ENJL model [2] can be affected by two additional contributions: the next to leading corrections in the inverse cutoff expansion and the gluonic corrections. Motivated by the necessity of reaching a highly accurate theoretical prediction of the hadronic contribution to the muon $g-2$, we study in detail both the effects.

Short Title: The muon $g-2$ in the Quark-Resonance model.

Work partially supported by the EEC Human Capital and Mobility program.

PACS.: 12.40.Aa

(Submitted to Phys. Lett. A)

* email: pallante@vaxtov.roma2.infn.it
fax: ++39-6-9403-427

Effective chiral Lagrangians *à la* Nambu-Jona Lasinio are a good theoretical framework to understand the hadronic vacuum polarization contribution to the anomalous magnetic moment of the muon, given by the diagram in Figure 1.

Phenomenological estimates of $a_\mu^h = (g^h - 2)/2$ are obtained from the best fit of the $e^+e^- \rightarrow \text{hadrons}$ total cross section $\sigma^h(t)$ through the usual dispersion relation

$$a_\mu^h = \frac{1}{4\pi^3} \int_{4m_\pi^2}^{\infty} dt K(t) \sigma^h(t), \quad (1)$$

whith the QED function $K(t)$ given by:

$$K(t) = \int_0^1 dx \frac{x^2(1-x)}{x^2 + (1-x)t/m_\mu^2}. \quad (2)$$

The most recent numerical estimates give the following values:

$$\begin{aligned} &\bullet 7.07(.066)(.17) \cdot 10^{-8} \quad [3] \\ &\bullet 6.84(.11) \cdot 10^{-8} \quad [4] \\ &\bullet 7.100(.105)(.49) \cdot 10^{-8} \quad [5], \end{aligned} \quad (3)$$

where the first error is statistical and the second one is systematic. In what follows we give a theoretical picture to understand the above numerical values.

a_μ^h is related to the renormalized hadronic photon self-energy $\Pi_R^h(Q^2)$ through the following integral [2, 6]

$$a_\mu^h = \frac{\alpha}{\pi} \int_0^1 dx (1-x) \left[-e^2 \Pi_R^h \left(\frac{x^2}{1-x} m_\mu^2 \right) \right]. \quad (4)$$

$\Pi_R^h(Q^2)$ is given in terms of the vector two point function $\Pi_V^1(Q^2)$ which has been extensively analyzed in refs. [1, 7]:

$$\Pi_R^h(Q^2) = \sum_{i=u,d,s} Q_i^2 (\Pi_V^1(Q^2) - \Pi_V^1(0)) = \frac{2}{3} (\Pi_V^1(Q^2) - \Pi_V^1(0)), \quad (5)$$

where $Q_i = (2/3, -1/3, -1/3)$ are the charges of the SU(3) flavour quarks u,d,s and the renormalized photon self-energy satisfies the constraint $\Pi_R^h(0) = 0$.

Because the typical momenta of the off-shell photons are of the order of the squared muon mass ($Q^2 \sim .01 \text{GeV}^2$) the integral is dominated by the low energy contribution to $\Pi_R^h(Q^2)$. By doing the Taylor expansion of $\Pi_R^h(Q^2)$ at $Q^2 = 0$ and by imposing $\Pi_R^h(0) = 0$ one has

$$\Pi_R^h(Q^2) = Q^2 \Pi_R^{h'}(Q^2) = Q^2 \left[\frac{d\Pi_R^h}{dQ^2}(0) + \frac{1}{2} Q^2 \frac{d^2\Pi_R^h}{(dQ^2)^2}(0) + \dots \right]. \quad (6)$$

Notice that $\Pi_R^{h'}(Q^2)$ coincides with the first derivative only at $Q^2 = 0$. The term with the second derivative contains one additive power of the ratios Q^2/Λ_χ^2 and Q^2/M_Q^2 , where $\Lambda_\chi \sim 1$ GeV is the ultraviolet low-energy cutoff and $M_Q \sim 300$ MeV is the infrared low-energy cutoff and are the natural dimensionful parameters of the long-distance expansion.

By first approximation $\Pi_R^h(Q^2) \sim Q^2 \frac{d\Pi_R^h}{dQ^2}(0)$ and the integral of eq. (4) gives the value for a_μ^h

$$a_\mu^h = \left(\frac{\alpha}{\pi}\right)^2 m_\mu^2 \frac{4\pi^2}{3} \left[-\frac{2}{3} \frac{d\Pi_V^1}{dQ^2}(0) \right]. \quad (7)$$

The calculation of a_μ^h reduces then to the calculation of the first derivative of the vector two-point function at $Q^2 = 0$, as was already pointed out in ref. [2]. In ref. [7] the long-distance behaviour of the vector function was derived in the ENJL framework. In [1] we have shown that the inclusion in the bosonized NJL Lagrangian of higher dimensional quark-resonance vertices, which are suppressed respect to the leading lowest dimensional four-quark operator by powers of the inverse cutoff Λ_χ , generates next-to-leading power corrections to the leading logarithms (NPLL) of the parameters of the effective resonance Lagrangian which are responsible of their Q^2 dependence.

As a consequence, higher dimensional quark-resonance operators modify the long distance behaviour of the vector Green's function predicted by the ENJL model and enter in the determination of a_μ^h through eq. (4). Already in the first approximation of eq. (7) the NPLL corrections proportional to Q^2 , i.e. of the type $Q^2/\Lambda_\chi^2 \ln(\Lambda_\chi^2/M_Q^2)$ give contribution to the derivative at $Q^2 = 0$; the derivative at $Q^2 = 0$ is sensitive to the behaviour at shorter distances.

We proceed as follows. Using the first approximation of eq. (7) we review the ENJL prediction already derived in [2]. Then we study the relevance of two sources of corrections: the NPLL contributions and the gluon contributions. Beyond the first approximation we analyze the sensitivity to both of them via the evaluation of the dispersive integral of eq. (4) over the long-distance part of $\Pi_R^h(Q^2)$.

The vector two-point function in the ENJL model and in the chiral limit can be parametrized in terms of the running photon-vector coupling $f_V(Q^2)$ and the squared mass of the vector resonance $M_V^2(Q^2)$, as follows:

$$\Pi_V^1(Q^2) = \frac{2f_V^2(Q^2)M_V^2(Q^2)}{M_V^2(Q^2) + Q^2}, \quad (8)$$

or equivalently in terms of the vector two-point function in the mean field approximation $\bar{\Pi}_V^1(Q^2)$ [7]

$$\Pi_V^1(Q^2) = \frac{\bar{\Pi}_V^1(Q^2)}{1 + Q^2 \frac{8\pi^2 G_V}{N_c \Lambda_\chi^2} \bar{\Pi}_V^1(Q^2)}, \quad (9)$$

where $G_V(\Lambda_\chi)$ is the coefficient of the four-quark vector-like interaction in the ENJL Lagrangian. The Q^2 dependent parameters are given by:

$$\begin{aligned} \bar{\Pi}_V^1(Q^2) &= \frac{N_c}{16\pi^2} 8 \int_0^1 d\alpha \alpha(1-\alpha) \Gamma(0, \alpha Q) \\ f_V^2(Q^2) &= \frac{1}{2} \bar{\Pi}_V^1(Q^2) \\ M_V^2(Q^2) &= \frac{N_c \Lambda_\chi^2}{8\pi^2 G_V} \left(\bar{\Pi}_V^1(Q^2) \right)^{-1}, \end{aligned} \quad (10)$$

with the incomplete Gamma function $\Gamma(0, \alpha Q) = -\ln \alpha Q - \gamma_E + \mathcal{O}(\alpha Q)$, $\alpha Q = (M_Q^2 + \alpha(1-\alpha)Q^2)/\Lambda_\chi^2$ and $\gamma_E = 0.5772\dots$ is the Euler's constant. Expressions (8) and (9) with the parameters (10) correspond to the diagram of Figure 2a, which is the infinite resummation of linear chains of constituent quark bubbles with the insertion of the leading four-quark vector operator of the ENJL Lagrangian. Linear chains of quark bubbles are of order N_c , while loops of chains of quark bubbles are of order 1 in the $1/N_c$ expansion.

The derivative at $Q^2 = 0$ is given by

$$\frac{d\Pi_V^1}{dQ^2}(0) = \frac{d\bar{\Pi}_V^1}{dQ^2}(0) - \bar{\Pi}_V^1(0)^2 \frac{8\pi^2 G_V}{N_c \Lambda_\chi^2} = 2 \frac{df_V^2}{dQ^2}(0) - 2 \frac{f_V^2(0)}{M_V^2(0)} \quad (11)$$

The ENJL model gives the following prediction:

$$\frac{d\Pi_V^1}{dQ^2}(0) = -\frac{N_c}{16\pi^2} \frac{1}{M_Q^2} \frac{4}{15} \left[e^{-\frac{M_Q^2}{\Lambda_\chi^2}} + \frac{5}{6} \frac{1-g_A}{g_A} \Gamma\left(0, \frac{M_Q^2}{\Lambda_\chi^2}\right) \right], \quad (12)$$

where g_A is the mixing parameter between the axial-vector and the pseudoscalar mesons in the bosonized ENJL action and it is related to the vector meson mass and the vector coupling G_V by the following relations [7]:

$$\frac{1 - g_A}{g_A} = 4M_Q^2 \frac{G_V}{\Lambda_\chi^2} \Gamma(0, M_Q^2/\Lambda_\chi^2) = \frac{6M_Q^2}{M_V^2}. \quad (13)$$

With the values of the best fit 1 of ref. [8] $M_Q = 265\text{MeV}$, $\Lambda_\chi = 1.165\text{GeV}$ and $g_A = 0.61$ we obtain for a_μ^h the value $a_\mu^h = 8.66 \cdot 10^{-8}$, which corresponds to the value $\frac{d\Pi_V^1}{dQ^2}(0) = -0.164$ of the first derivative. In formula (12) the incomplete Gamma function has been approximated to its leading logarithmically divergent part. This corresponds to the substitutions $\Gamma(0, \alpha_Q) = -\ln \alpha_Q - \gamma_E$ and $\exp(-M_Q^2/\Lambda_\chi^2) = 1$, where $\exp(-M_Q^2/\Lambda_\chi^2)$ comes from the derivative of $\Gamma(0, \alpha_Q)$ at $Q^2 = 0$.

Chiral loop corrections due to π, K exchanges, are not included in the above value of a_μ^h . They are given by the diagram in Figure 2b and are next-to-leading (i.e. $O(1)$) in the $1/N_c$ expansion; in the ENJL framework they are generated by diagrams with loops of chains of quark bubbles. This contribution has been derived in [2] using *ChPt* with a value of $(0.71 \pm 0.07) \cdot 10^{-8}$. The two summed contributions give

$$a_\mu(\text{had}) = a_\mu(\text{Fig. 2a}) + a_\mu(\chi\text{loops}) = 9.37 \cdot 10^{-8}, \quad (14)$$

which is a rather high value compared to the phenomenological estimates in (3). Beyond the fact that the first derivative approximation can be not sufficiently accurate, we first analyze the effects of the two “extra” contributions we have mentioned.

The first source of “extra” corrections can be derived in the framework of the Quark-Resonance model formulated in [1].

The vector two-point function calculated with the inclusion of NTL vertices corresponds to the diagram of Figure 2c.: the vector resonance exchange diagram plus the “local” diagram. The infinite resummation of linear chains of quark bubbles of Figure 2a is a part of the contributions to the renormalized vector resonance propagator.

The complete set of NTL corrections (i.e. $1/\Lambda_\chi^2$), includes two types of contributions [1]:

- I. NTL genuine power corrections (NTLP) of the type: $\frac{Q^2}{\Lambda_\chi^2}, \frac{M_Q^2}{\Lambda_\chi^2}$
- II. NTL power corrections to the leading logs (NPLL) of the type: $\frac{Q^2}{\Lambda_\chi^2} \ln \alpha_Q, \frac{M_Q^2}{\Lambda_\chi^2} \ln \alpha_Q$.

Class I is generated by an infinite number of higher dimensional quark-resonance vertices, while class II is generated by a finite number of $1/\Lambda_\chi^2$ vertices [1]. A

best fit to the experimental $e^+e^- \rightarrow \text{hadrons}$ cross section in the $I = 1, J = 1$ channel and in the intermediate Q^2 region (500 MeV - 900 MeV) has shown the numerical relevance of the new NPLL counterterms proportional to Q^2 [1], while NPLL corrections proportional to the IR cutoff M_Q are negligible in this regime. They are not negligible when treating the very low energy behaviour ($Q^2 \rightarrow 0$) of the Green's functions, as it happens in the present case.

In table (1) the type of quark-resonance vertices we need are listed. We distinguish four sectors: the derivative one, the vector one, the scalar one and the scalar-vector one. NTL corrections proportional to Q^2 get contributions from the derivative and the vector sets, while NTL corrections proportional to M_Q^2 get contributions also from the scalar and scalar-vector sets when the scalar field assumes its VEV, $\langle H \rangle = M_Q$, which plays the role of the IR cutoff of the effective theory.

The full running of the vector resonance parameters ($Z_V =$ vector wave function renormalization constant, $f_V =$ vector-photon coupling and $M_V =$ vector mass) is parametrized as follows:

$$\begin{aligned}
 Z_V(Q^2) &= \frac{N_c}{16\pi^2} \frac{1}{3} \int_0^1 d\alpha \Gamma(0, \alpha_Q) \left[6\alpha(1-\alpha) + 12\alpha(1-\alpha)\beta_V^1 \frac{Q^2}{\Lambda_\chi^2} + \beta_M^1 \frac{M_Q^2}{\Lambda_\chi^2} P_1(\alpha) \right] \\
 M_V^2(Q^2) &= \frac{N_c}{16\pi^2} \frac{\Lambda_\chi^2}{2\tilde{G}_V} \frac{1}{Z_V} \left[1 + \beta_M^2 \frac{M_Q^2}{\Lambda_\chi^2} \int_0^1 d\alpha \Gamma(0, \alpha_Q) P_2(\alpha) \right] \\
 f_V(Q^2) &= \frac{1}{\sqrt{Z_V}} \frac{N_c}{16\pi^2} \frac{\sqrt{2}}{3} \int_0^1 d\alpha \Gamma(0, \alpha_Q) \left[6\alpha(1-\alpha) + 6\alpha(1-\alpha)\beta_\Gamma^1 \frac{Q^2}{\Lambda_\chi^2} + \right. \\
 &\quad \left. 6\alpha(1-\alpha)\beta_V^1 \frac{Q^2}{\Lambda_\chi^2} + \beta_M^3 \frac{M_Q^2}{\Lambda_\chi^2} P_3(\alpha) \right]. \tag{15}
 \end{aligned}$$

In the calculation of f_V and Z_V we have not included NTLP corrections. They give a correction which is almost 1% of the leading logarithmic term. Genuine power corrections can be generated by the quadratically or more divergent part of diagrams that contain higher dimensional vertices which are suppressed by inverse powers of the UV cutoff Λ_χ .

NTLP corrections to the squared vector mass and proportional to M_Q can be reabsorbed in the renormalization of the vector coupling G_V as follows:

$$\frac{\Lambda_\chi^2}{\tilde{G}_V} = \frac{\Lambda_\chi^2}{G_V} \left[1 + \delta' \frac{M_Q^2}{\Lambda_\chi^2} \right]. \tag{16}$$

In eq. (15) the dependence upon the Feynman parameter α is always of the form

$\alpha(1-\alpha)$ for the Q^2/Λ_x^2 corrections. The polynomials $P_i(\alpha)$ are explicitly calculable for each NPLL counterterm. We will put them equal to the leading polynomial $\alpha(1-\alpha)$ which is still a good approximation. With this assumption the three vector parameters Z_V , M_V^2 and f_V^2 at $Q^2 = 0$ are given by:

$$\begin{aligned} Z_V(0) &= \frac{N_c}{16\pi^2} \frac{1}{3} \Gamma(0, M_Q^2/\Lambda_x^2) \left[1 + \frac{\beta_M^1 M_Q^2}{6 \Lambda_x^2} \right] \\ M_V^2(0) &= \frac{N_c}{16\pi^2} \frac{\Lambda_x^2}{2\tilde{G}_V} \frac{1}{Z_V(0)} \left[1 + \frac{\beta_M^2 M_Q^2}{6 \Lambda_x^2} \Gamma(0, M_Q^2/\Lambda_x^2) \right] \\ f_V^2(0) &= \frac{2}{9} \frac{1}{Z_V(0)} \left(\frac{N_c}{16\pi^2} \right)^2 \Gamma^2(0, M_Q^2/\Lambda_x^2) \left[1 + \frac{\beta_M^3 M_Q^2}{6 \Lambda_x^2} \right]^2. \end{aligned} \quad (17)$$

The NPLL corrections proportional to M_Q^2 do modify the ENJL leading prediction of the parameters of the effective meson Lagrangian at zero energy. One way to estimate the new coefficients β_M^i , is to do the best fit of the whole set of the leading (M_Q, Λ_x, g_A) and NPLL parameters (with and without gluonic corrections) at $Q^2 = 0$ using as inputs the experimental values of the low energy meson parameters; although a sufficiently accurate determination of the β_M^i is still not accessible with the present uncertainty on the very low energy experimental data.

The ratio f_V^2/M_V^2 and the derivative of the squared coupling at $Q^2 = 0$, which enter in eq. (11), are given by the following expressions and retaining up to $1/\Lambda_x^2$ terms:

$$\begin{aligned} \frac{f_V^2(0)}{M_V^2(0)} &= \frac{2}{3} \frac{N_c}{16\pi^2} \frac{1}{M_V^2(0)^{ENJL}} \Gamma(0, M_Q^2/\Lambda_x^2) \left[1 + \frac{\beta_M^3 M_Q^2}{3 \Lambda_x^2} - \frac{\beta_M^2 M_Q^2}{6 \Lambda_x^2} \Gamma(0, M_Q^2/\Lambda_x^2) \right] \\ f_V^2(0) &= \frac{2}{3} \frac{N_c}{16\pi^2} \left\{ \Gamma(0, M_Q^2/\Lambda_x^2) \frac{2\beta_\Gamma^1}{\Lambda_x^2} - \frac{1}{5M_Q^2} e^{-M_Q^2/\Lambda_x^2} \left[1 + \frac{2\beta_M^3 - \beta_M^1 M_Q^2}{6 \Lambda_x^2} \right] \right\}. \end{aligned} \quad (18)$$

Again the approximation $\Gamma(0, \alpha_Q) = -\ln \alpha_Q - \gamma_E$ and $\exp(-M_Q^2/\Lambda_x^2) = 1$ is understood and we have used the relation of eq. (13) which defines $M_V^2(0)^{ENJL}$. We assume its numerical value given by the fit 1 of ref. [8] which is $(0.811)^2 \text{ GeV}^2$.

The size of the Q^2 corrections has been determined by the best fit of ref. [1]:

$$\beta_\Gamma^1 = -0.75 \pm 0.01 \quad \beta_V^1 = -0.79 \pm 0.01. \quad (19)$$

The sign of $\beta_\Gamma^1, \beta_V^1$ is negative and increases the value of a_μ^h . By including only Q^2 type corrections the value of a_μ^h increases to $1.22 \cdot 10^{-7}$. Comparable values of the

β_M^i coefficients give as a maximum range of variation of a_μ^h $1.20 \cdot 10^{-7} \div 1.24 \cdot 10^{-7}$. This proves that Q^2 dependent contributions give the bulk of the NPLL corrections to a_μ^h calculated within the first derivative approximation.

Gluonic corrections can be parametrized following ref. [7]. The leading contribution in the $1/N_c$ expansion involves only one unknown parameter g which is related to the lowest dimensional gluon vacuum condensate:

$$g = \frac{\pi^2}{6N_c M_Q^4} \langle \frac{\alpha_s}{\pi} GG \rangle. \quad (20)$$

Because $\langle \frac{\alpha_s}{\pi} GG \rangle$ is $O(N_c)$ g is $O(1)$ and the leading gluonic correction to the two-point vector function is still $O(N_c)$. The role of gluonic corrections in effective low energy fermion models is still an unsolved theoretical problem. What is clear is that the two gluon condensate of eq. (20) is only the low energy ($< \Lambda_\chi$) ‘residue’ of the standard two gluon condensate which is phenomenologically estimated through QCD sum rules. The latter suggest an $O(1)$ g parameter, while best fits of the ENJL parameters, using as inputs the experimental values of f_π, L_i and the meson resonances’ parameters [8], strongly favour a value of $g \leq 0.5$. The first phenomenological estimation, usually referred to as the “standard value”, has been obtained by Shifman et al. (SVZ) [9] by studying the charmonium channel and using Operator Product Expansion: they obtain $\langle \frac{\alpha_s}{\pi} GG \rangle = 0.012 \text{ GeV}^4$ (i.e. $g=1.3$). A compatible value $\langle \alpha_s GG \rangle = (3.9 \pm 1.0)10^{-2} \text{ GeV}^4$ has been obtained [10] from the $e^+e^- \rightarrow I = 1$ hadron cross section and using moment sum rules ratio. The most recent estimation via FESR (Finite Energy sum rules) [11] gives a significative higher value $\langle \frac{\alpha_s}{\pi} GG \rangle = 0.044_{-0.021}^{+0.015} \text{ GeV}^4$ (i.e. $g \sim 4.8$), although the error in all cases has to be conservatively taken around 40%.

In what follows we will use three values of g which are acceptable in the ENJL model. The IR cutoff M_Q , the UV cutoff Λ_χ and the axial-pseudoscalar mixing parameter g_A , extracted from the best fits of experimental data, vary as functions of g as it is summarized in table (2). M_Q decreases sensitively by increasing g .

Leading gluonic corrections can be expressed as an additive contribution to the function $\bar{\Pi}_V^1(Q^2)$ which is written for $N_c = 3$ as [12]

$$\bar{\Pi}_V^{1g}(Q^2) = \frac{3gM_Q^4}{2\pi^2Q^4}(-1 + 3\mathcal{I}_2 - 2\mathcal{I}_3), \quad (21)$$

in terms of the Q^2 dependent functions

$$\tau_N = \int_0^1 d\alpha \frac{1}{[1 + \frac{Q^2}{M_Q^2} \alpha(1 - \alpha)]^N}. \quad (22)$$

Expanding at small Q^2 we obtain their values at $Q^2 = 0$:

$$\bar{\Pi}_V^{1g}(0) = -\frac{3g}{20\pi^2} \quad \bar{\Pi}_V'^{1g}(0) = \frac{6g}{70\pi^2 M_Q^2}, \quad (23)$$

which give the following expression for the derivative:

$$\begin{aligned} \frac{d\Pi_V^1}{dQ^2}(0) &= \frac{d\Pi_V^{1g=0}}{dQ^2}(0) + \Delta^g \\ \Delta^g &= \frac{6g}{70\pi^2 M_Q^2} - \left(\frac{3g}{20\pi^2}\right)^2 \frac{8\pi^2 G_V}{N_c \Lambda_\chi^2} \left(1 - \frac{40\pi^2}{3g} \Pi_V^{1g=0}(0)\right). \end{aligned} \quad (24)$$

Notice that $\Pi_V^{1g=0}(0) = \bar{\Pi}_V^{1g=0}(0)$; all the quantities with superscript $g = 0$ are those at $g=0$ with the parameters M_Q , Λ_χ and g_A rescaled according to table (2) for a given g in formula (24). In table (3) we give the gluonic corrections to the derivative at $Q^2 = 0$ with $g = 0.25, 0.5$.

Gluonic contributions decrease a_μ^h towards a better agreement with the phenomenological estimates (3).

The evaluation of the full dispersive integral (4) requires the knowledge of the long distance (ld) plus the short distance (sd) behaviour of $\Pi_R^h(Q^2)$. We can do our best performing the matching between the ld prediction coming from the effective theory and the sd prediction coming from perturbative QCD. In ref. [2] a value of a_μ^h (*Fig.2a*) $= 6.7 \cdot 10^{-8}$ has been obtained in the ENJL framework with a best fitted matching point $\hat{x} \simeq 0.91$ which corresponds to an euclidean $\hat{Q}^2 = \hat{x}^2 / (1 - \hat{x}) m_\mu^2 \simeq (320)^2 \text{ MeV}^2$. The value obtained for a_μ^h is quite better than the first approximation value $8.66 \cdot 10^{-8}$.

To see how “extra” corrections modify the ENJL prediction is sufficient to study the integral (4) over the ld part in the range $\int_0^{\hat{x}}$ for different values of \hat{x} corresponding to an equivalent value of $\hat{Q}^2 = (0.3)^2, (0.5)^2, (0.8)^2 \text{ GeV}^2$.

NPLL corrections proportional to Q^2 in the QR model lead to a vector two-point function which decreases faster in Q^2 than the ENJL prediction. The dispersive integral gives for a_μ^h the values of table (4).

The correction induced by higher order terms proportional to Q^2 and which are relevant in the intermediate Q^2 region is about one percent. This proves that a_μ^h is

practically only sensitive to perturbative corrections which modify the very low Q^2 region, i.e. $Q^2 \leq (500\text{MeV})^2$.

Gluonic corrections modify the ENJL vector two-point function for all Q^2 as shown in figure 3. They modify the ENJL prediction of a_μ^h as summarized in table (5). The corrections are 10% for $g=0.5$ and 15% for $g=0.25$. They decrease a_μ^h . A better determination of non-gluonic contributions to a_μ^h can be used to constrain the value of the g parameter in low energy effective fermion models.

We conclude that the ENJL prediction is reliable within 30%. Both gluonic corrections and next-to-leading higher dimensional quark-resonance interactions have to be taken into account if one wants to reach an accuracy better than 30%. The first derivative approximation is not sufficiently accurate to estimate the hadronic vacuum polarization contribution to a_μ^h , although the quantity is sensitive only to “extra” corrections in the low Q^2 region ($Q < 500$ MeV). NPLL corrections proportional to Q^2 do not affect a_μ^h . NPLL corrections proportional to M_Q^2 and gluonic corrections are relevant in the low Q^2 region. Their inclusion can explain the full agreement of the ENJL prediction with the phenomenological estimates (3) of a_μ^h .

Acknowledgements. I am grateful to Eduardo de Rafael for having called my attention to this problem and for useful discussions.

FIGURE CAPTIONS

- 1) Hadronic vacuum polarization diagram to the anomalous magnetic moment of the muon.
- 2a) The vector two-point function in the ENJL model and leading in the $1/N_c$ expansion. It is given by the infinite resummation of linear chains of constituent quark bubbles; each four-quark vertex is the leading vertex of the ENJL model with coupling G_V .
- 2b) Chiral loops corrections to the vector two-point function. They are of $O(1)$ (i.e. next-to-leading) in the $1/N_c$ expansion and in the ENJL model they are generated by the infinite resummation of loops of chains of constituent quark bubbles.
- 2c) The vector two-point function in the QR model and leading in the $1/N_c$ expansion. It is given by the “local” diagram and the vector-exchange diagram with the renormalized vector meson propagator. The diagram of figure 2a is a part of the contribution to the renormalized vector meson propagator.
- 3) The vector two-point function $\Pi_V^1(Q^2)$ in the ENJL model without gluonic corrections (solid line) and with gluonic corrections for $g=0.25, 0.5$ (dashed lines).

TABLE CAPTIONS

- 1) $1/\Lambda_\chi^2$ quark-resonance vertices of the sectors: I) derivative, II) vector, III) scalar and IV) scalar-vector which give contribution to the NPLL corrections.
- 2) Values of M_Q , Λ_χ and g_A of the ENJL model obtained from the best fits of ref. [8] to the experimental data of low energy parameters and with fixed values of the gluonic parameter $g=0, 0.25, 0.5$.
- 3) Gluonic corrections to a_μ^h in the first derivative approximation for two values of the gluonic parameter g favoured by the ENJL model. Δ^g is the gluonic correction to the first derivative as defined in eq. (24), $d\Pi_V^1/dQ^2(0)$ is the first derivative including gluonic corrections. In the last two columns the numerical value of a_μ^h and the variation in percentage are shown.

- 4) Numerical values of a_μ^h obtained through the dispersion relation (4), where the integral is performed on the long-distance part of Π_R^h predicted by the QR model in the range $0 < Q^2 < \hat{Q}^2$ and compared to the ENJL prediction.
- 5) Numerical values of a_μ^h obtained through the dispersion relation (4), where the integral is performed on the long-distance part of Π_R^h predicted by the ENJL model in the range $0 < Q^2 < \hat{Q}^2$ without the inclusion of gluonic corrections ($g=0$) and including gluonic corrections with $g=0.25, 0.5$.

References

- [1] E. Pallante and R. Petronzio, Preprint ROM2F 37/93, submitted to Nucl. Phys. B
- [2] E. de Rafael, *Phys. Lett.* **B322** (1994) 239.
- [3] T. Kinoshita, B. Nizić and Y. Okamoto, *Phys. Rev.* **D31** (1985) 2108.
- [4] J.A. Casas, C. Lopez and F.J. Ynduráin, *Phys. Rev.* **D32** (1985) 736.
- [5] L.M. Kurdadze et al., *Sov. J. Nucl. Phys.* **40** (1984) 286.
- [6] B.E. Lautrup, A. Peterman and E. de Rafael, *Phys. Rep.* **3C** (1972) 193.
- [7] J. Bijnens, E. de Rafael and H. Zheng, Preprint CERN-TH 6924/93, CTP-93/P2917, NORDITA-93/43 N,P.
- [8] J. Bijnens, C. Bruno and E. de Rafael, *Nucl. Phys.* **B390** (1993) 501.
- [9] M.A. Shifman, A.I. Vainshtein and V.I. Zakharov, *Nucl. Phys.* **B147** (1979) 385, 448.
- [10] G. Launer, S. Narison and R. Tarrach, *Z. Phys.* **C 26** (1984) 433.
- [11] R.A. Bertlmann et al., *Z. Phys.* **C 39** (1988) 231.
- [12] S. Narison, “QCD Spectral Sum Rules”, World Scientific Lecture Notes in Physics, Vol. 26.

DERIVATIVE

$$\beta_1^1 \bar{Q} \gamma_\nu d^\mu \Gamma_{\mu\nu} Q + \beta_1^2 \bar{Q} \gamma_\mu \{\bar{d}^\mu, \bar{d}^2\} Q$$

VECTOR

$$\begin{aligned} & \beta_V^1 \bar{Q} \gamma_\mu d^2 W_\mu^+ Q + \beta_V^2 \bar{Q} \gamma_\mu \{W_\mu^+, \bar{d}^2\} Q + \beta_V^3 \bar{Q} \gamma_\mu \{\{\bar{d}_\mu, \bar{d}_\nu\}, W_\nu^+\} Q + \beta_V^4 \bar{Q} \gamma_\mu [\Gamma_{\mu\nu}, W_\nu^+] Q + \\ & \beta_V^5 \bar{Q} \gamma_\mu \{W^{+2}, \bar{d}^\mu\} Q + \beta_V^6 \bar{Q} \gamma_\mu [d^\mu W_\nu^+, W_\nu^+] Q + \beta_V^7 \bar{Q} \gamma_\mu (W_\mu^+ W_\nu^+ \bar{d}_\nu + \bar{d}_\nu W_\nu^+ W_\mu^+) Q + \\ & \beta_V^8 \bar{Q} \gamma_\mu (W_\nu^+ W_\mu^+ \bar{d}_\nu + \bar{d}_\nu W_\mu^+ W_\nu^+) Q + \beta_V^9 \bar{Q} \gamma_\mu [d^\nu W_\mu^+, W_\nu^+] Q \end{aligned}$$

SCALAR

$$\beta_S^1 \bar{Q} H^3 Q + \beta_S^2 \bar{Q} \gamma_\mu \{H^2, \bar{d}^\mu\} Q + \beta_S^3 \bar{Q} \{H, \bar{d}^2\} Q$$

SCALAR-VECTOR

$$\begin{aligned} & \beta_{SV}^1 \bar{Q} \{W^{+2}, H\} Q + \beta_{SV}^2 \bar{Q} W_\mu^+ H W_\mu^+ Q + \beta_{SV}^3 \bar{Q} \gamma_\mu \{H^2, W_\mu^+\} Q + \beta_{SV}^4 \bar{Q} \gamma_\mu H W_\mu^+ H Q \\ & + \beta_{SV}^5 \bar{Q} (W_\mu^+ H \bar{d}_\mu + \bar{d}_\mu H W_\mu^+) Q + \beta_{SV}^6 \bar{Q} (H W_\mu^+ \bar{d}_\mu + \bar{d}_\mu W_\mu^+ H) Q. \end{aligned}$$

Table 1:

The covariant derivative of the vector field W_μ^+ and the scalar field H is defined as $d_\mu \mathcal{O} = \partial_\mu \mathcal{O} + [\Gamma_\mu, \mathcal{O}]$, while the covariant derivative on the *constituent* quark field Q is defined as $d_\mu Q = \partial_\mu Q + \Gamma_\mu Q$. $\Gamma_\mu = 1/2(\xi^\dagger \partial_\mu \xi + \xi \partial_\mu \xi^\dagger)$ is the vector current constructed with the square root of the pseudoscalar meson field $U = \xi^2 = \exp(i\phi/f_\pi)$. The identity $\Gamma_{\mu\nu} = -\frac{i}{2} f_{\mu\nu}^+ + \frac{1}{4} [\xi_\mu, \xi_\nu]$ introduces the field strength of the electromagnetic field $f_{\mu\nu}^+ = \xi F_{\mu\nu} \xi^\dagger + \xi^\dagger F_{\mu\nu} \xi$ which generates the photon-vector interaction associated with the coupling f_V .

g	M_Q (MeV)	Λ_χ (GeV)	g_A
$g = 0$	265	1.165	0.61
$g = 0.25$	246	1.062	0.62
$g = 0.5$	204	1.090	0.66

Table 2:

g	Δ^g	$d\Pi_V^1/dQ^2(0)$	a_μ^h	$\Delta a_\mu/a_\mu(\%)$
$g = 0.25$	0.048	-0.136	$7.2 \cdot 10^{-8}$	-17%
$g = 0.5$	0.134	-0.133	$7.0 \cdot 10^{-8}$	-19%

Table 3:

$\hat{Q}^2 \text{ GeV}^2$	$a_\mu^{QR} \times 10^8$	$a_\mu^{ENJL} \times 10^8$
$(0.5)^2$	6.9	6.8
$(0.8)^2$	7.3	7.1

Table 4:

$\hat{Q}^2 \text{ GeV}^2$	$a_\mu^h \text{ g}=0$	$a_\mu^h \text{ g}=0.25$	$a_\mu^h \text{ g}=0.5$
$(0.3)^2$	$5.9 \cdot 10^{-8}$	$5.0 \cdot 10^{-8}$	$5.3 \cdot 10^{-8}$
$(0.5)^2$	$6.8 \cdot 10^{-8}$	$5.9 \cdot 10^{-8}$	$6.3 \cdot 10^{-8}$
$(0.8)^2$	$7.1 \cdot 10^{-8}$	$6.2 \cdot 10^{-8}$	$6.6 \cdot 10^{-8}$

Table 5:

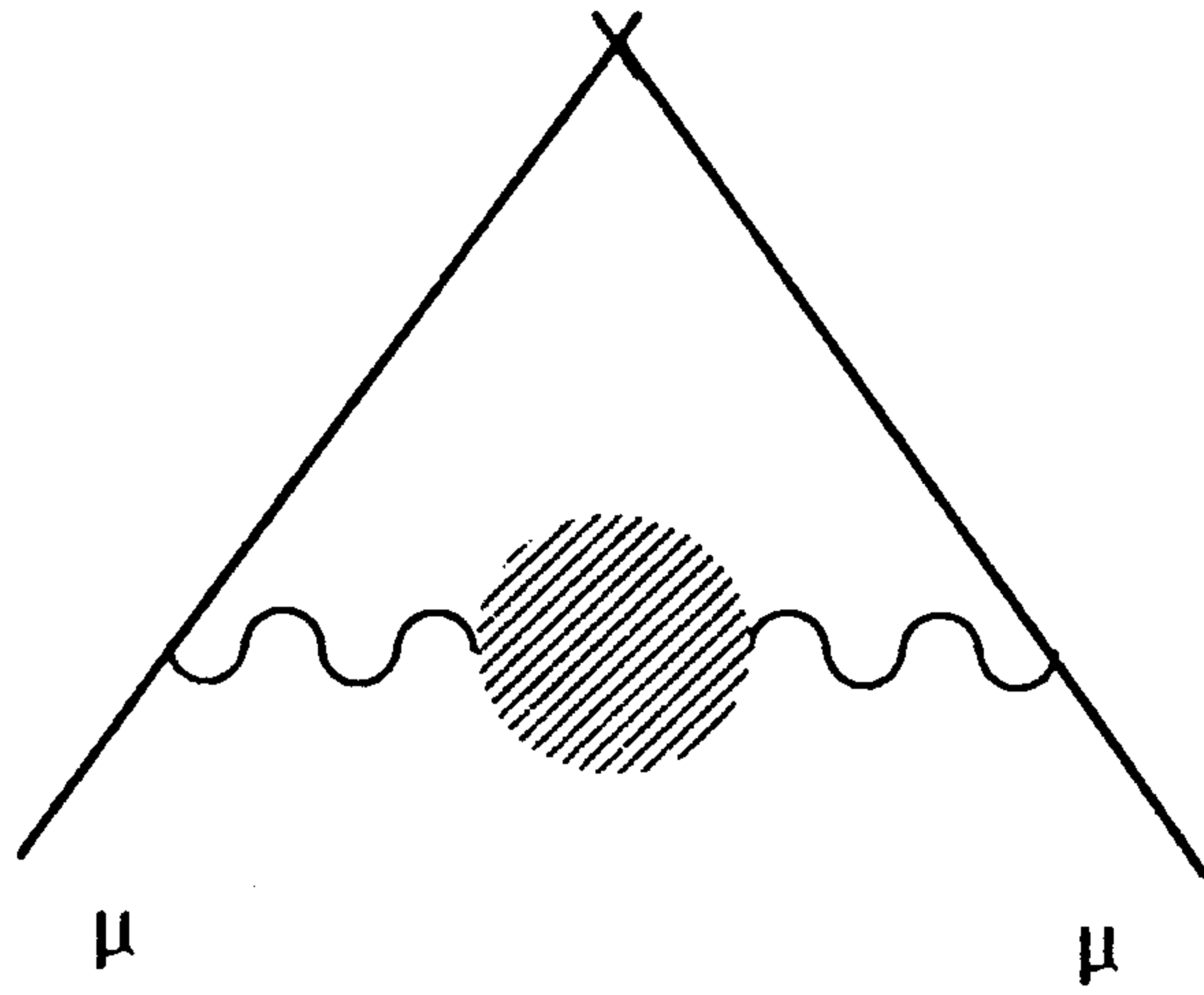


Fig. 1

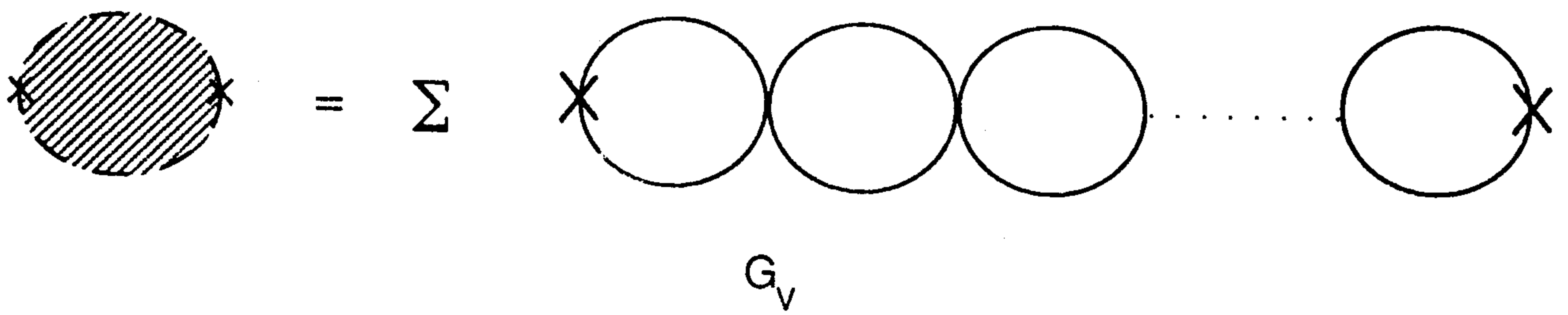
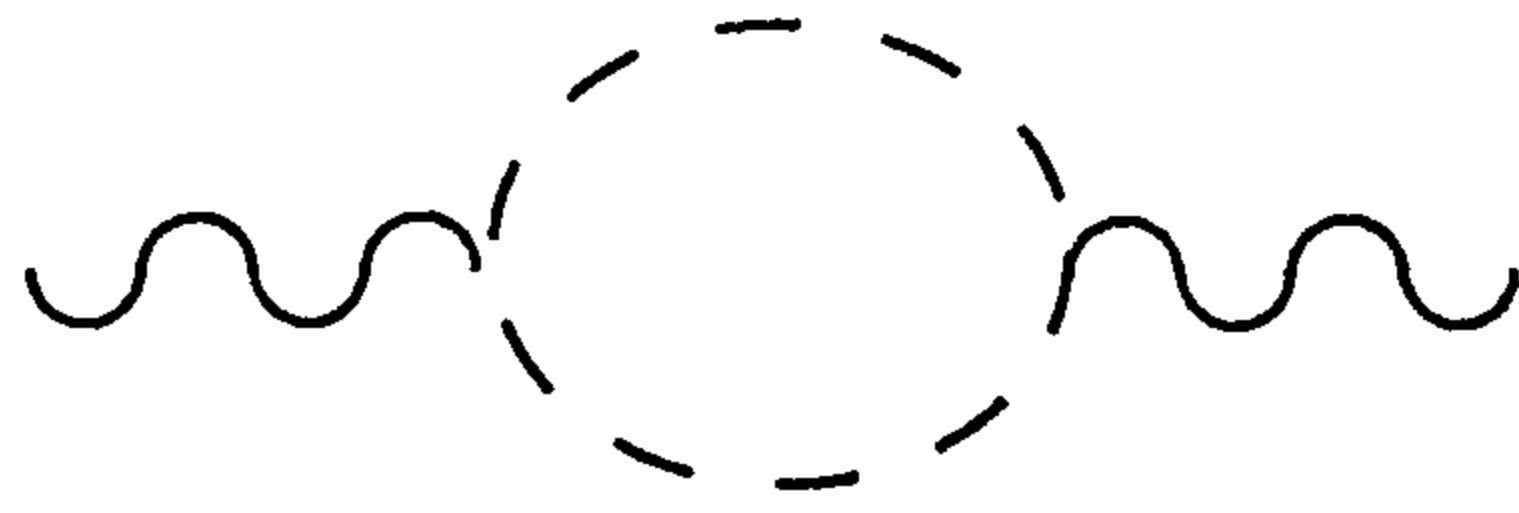


Fig. 2a



π, K

Fig. 2b

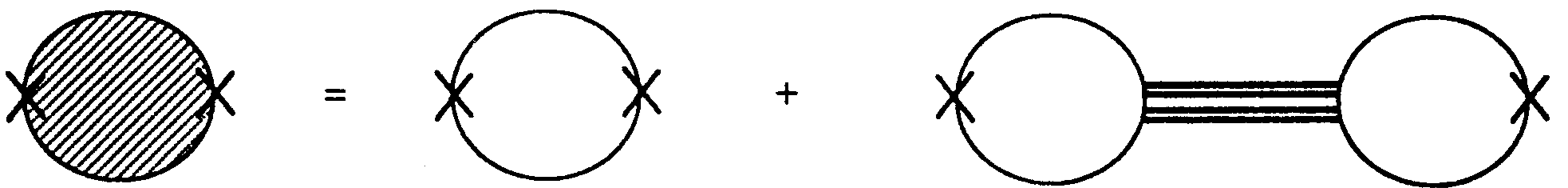


Fig. 2c

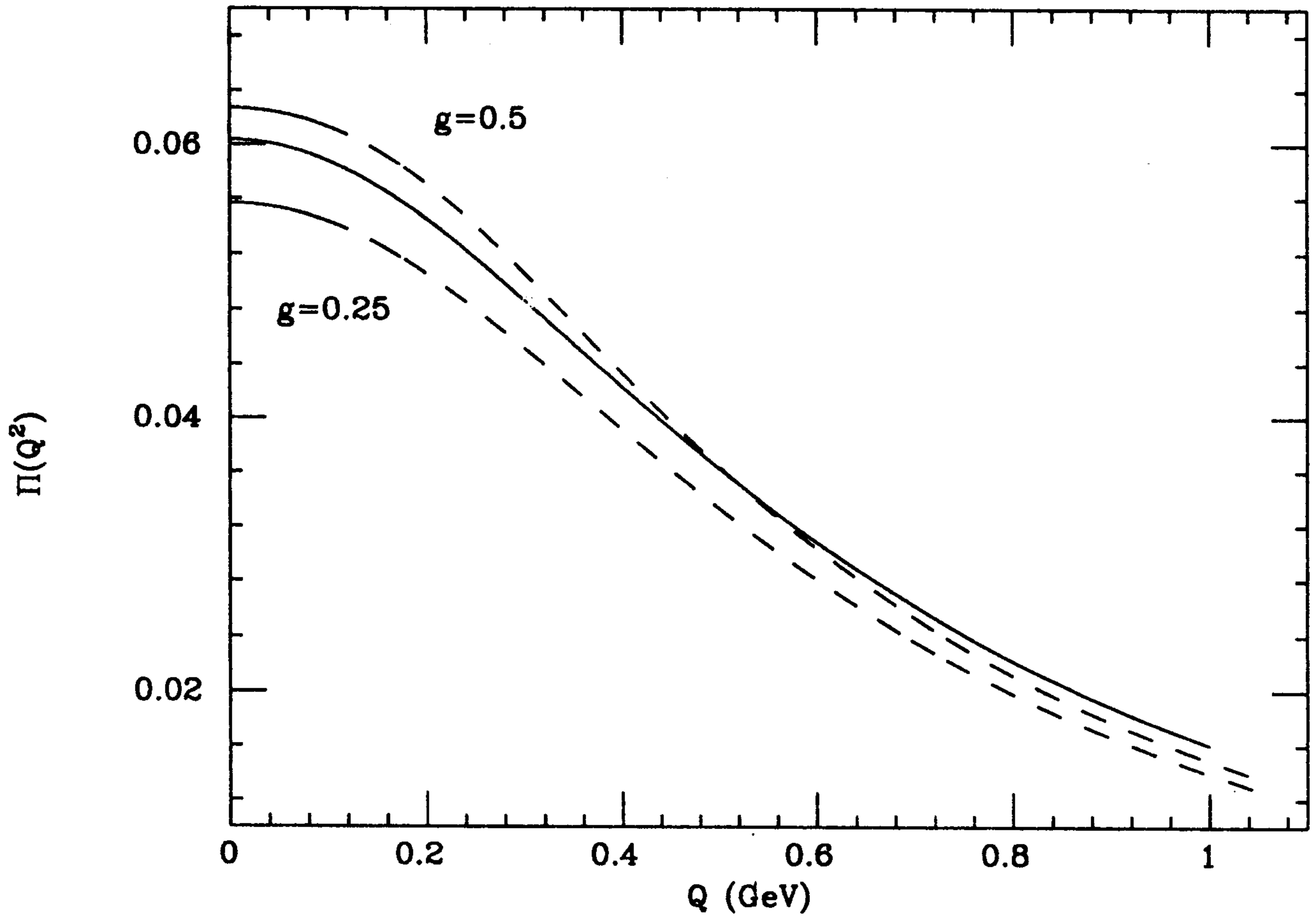


Fig. 3